HDLs in *apoA-I* transgenic *Abca1* knockout mice are remodeled normally in plasma but are hypercatabolized by the kidney

Ji-Young Lee,[1,*] Jenelle M. Timmins,[1,*] Anny Mulya,[*] Thomas L. Smith,[†] Yiwen Zhu,[§] Edward M. Rubin,[§] Jeffrey W. Chisholm,[**] Perry L. Colvin,[††] and John S. Parks[2,*]

Departments of Pathology* and Orthopedic Surgery,† Wake Forest University School of Medicine, Winston-Salem, NC 27157; Department of Genome Sciences,§ E. O. Lawrence Berkeley National Laboratory, Berkeley, CA 94720; Discovery Research,** CV Therapeutics, Inc., Palo Alto, CA, 94304; and Division of Gerontology,†† University of Maryland School of Medicine, and Geriatrics Research, Education, and Clinical Center, Baltimore Veterans Affairs Medical Center, Baltimore, MD 21201

Abstract **Patients homozygous for Tangier disease have a near absence of plasma HDL as a result of mutations in *ABCA1* and hypercatabolize normal HDL particles. To determine the relationship between ABCA1 expression and HDL catabolism, we investigated intravascular remodeling, plasma clearance, and organ-specific uptake of HDL in mice expressing the human apolipoprotein A-I (apoA-I) transgene in the *Abca1* knockout background. Small HDL particles (7.5 nm), radiolabeled with ^{125}I-tyramine cellobiose, were injected into recipient mice to quantify plasma turnover and the organ uptake of tracer. Small HDL tracer was remodeled to 8.2 nm diameter particles within 5 min in human apolipoprotein A-I transgenic (*hA-I^{Tg}*) mice (control) and knockout mice. Decay of tracer from plasma was 1.6-fold more rapid in knockout mice ($P < 0.05$) and kidney uptake was twice that of controls, with no difference in liver uptake. We also observed 2-fold greater hepatic expression of ABCA1 protein in *hA-I^{Tg}* mice compared with nontransgenic mice, suggesting that overexpression of human apoA-I stabilized hepatic ABCA1 protein in vivo. We conclude that ABCA1 is not required for in vivo remodeling of small HDLs to larger HDL subfractions and that the hypercatabolism of normal HDL particles in knockout mice is attributable to a selective catabolism of HDL apoA-I by the kidney.**—Lee, J-Y., J. M. Timmins, A. Mulya, T. L. Smith, Y. Zhu, E. M. Rubin, J. W. Chisholm, P. L. Colvin, and J. S. Parks. **HDLs in *apoA-I* transgenic *Abca1* knockout mice are remodeled normally in plasma but are hypercatabolized by the kidney. *J. Lipid Res.* 2005.** 46: **2233–2245.**

Supplementary key words apolipoprotein A-I • ATP binding cassette transporter A1 • high density lipoprotein

HDLs are the smallest of the plasma lipoprotein classes and contain as their major protein apolipoprotein A-I (apoA-I) (1). HDLs exhibit heterogeneity that can be demonstrated by density ultracentrifugation (2), size (3), mobility in an electrophoretic field (4), and apolipoprotein content (5). Interest in HDL metabolism is stimulated by the well-documented inverse correlation between plasma HDL cholesterol concentrations and coronary heart disease (6–8). Although several possible mechanisms for the atheroprotective effect of HDL have been proposed, most attention has been focused on the role of HDL in reverse cholesterol transport (RCT) as a mechanism for the movement of excess cholesterol mass from arterial foam cells back to the liver for secretion into bile (9).

The first step of the RCT pathway involves ABCA1-mediated transport of free cholesterol (FC) and phospholipid (PL) from cells to lipid-free or lipid-poor apoA-I, resulting in a nascent HDL particle that exhibits pre-β mobility on agarose gels (pre-β HDL) (10). More PL is added to the pre-β particle by phospholipid transfer protein (PLTP), and the FC is esterified to cholesteryl ester (CE) by LCAT, transforming a disc-shaped nascent HDL particle into an α-migrating spherical plasma HDL particle (11). Plasma HDL particles are also substrates for RCT and receive additional lipid through ABCG1-mediated cellular FC and PL efflux (12). The constant esterification of FC to CE also maintains a concentration gradient between cells and HDL particles for passive efflux of FC by aqueous diffusion (13).

Manuscript received 9 May 2005 and in revised form 5 July 2005.

Published, JLR Papers in Press, July 16, 2005.
DOI 10.1194/jlr.M500179-JLR200

Abbreviations: apoA-I, apolipoprotein A-I; CE, cholesteryl ester; EC, esterified cholesterol; FC, free cholesterol; FCR, fractional catabolic rate; FPLC, fast-protein liquid chromatography; *hA-I^{Tg}*, human apolipoprotein A-I transgenic; PL, phospholipid; PLTP, phospholipid transfer protein; RCT, reverse cholesterol transport; SR-BI, scavenger receptor class B type I; TC, tyramine cellobiose; WHAM, Wisconsin Hypoalpha Mutant.

[1] J-Y. Lee and J. M. Timmins contributed equally to this work.

[2] To whom correspondence should be addressed.
e-mail: jparks@wfubmc.edu

The addition and esterification of FC to HDL results in larger HDL subfractions that can be separated on nondenaturing gradient gels into small, medium, and large HDL particles that contain two, three, and four molecules of apoA-I per particle, respectively (14). These spherical HDL particles can deliver their CE content to the liver by whole particle uptake or by selective removal by scavenger receptor class B type I (SR-BI), which completes the RCT pathway (15). The available evidence suggests that the metabolism of HDL subfractions is intimately and intricately linked to the RCT pathway; therefore, a better understanding of HDL subfraction formation and catabolism will enhance our knowledge of RCT.

Tangier disease is a genetic disorder in which cells fail to assemble FC, PL, and apoA-I into nascent HDL particles as a result of mutations that inactivate *ABCA1*, resulting in a near absence of mature HDL particles in plasma and the accumulation of CE in macrophages in multiple tissues (16–19). Although much attention on the pathogenesis of Tangier disease has focused on the impairment of HDL biosynthesis caused by the absence of ABCA1, there is compelling evidence that the catabolism of plasma HDL particles is also affected. Radiolabeled plasma HDL tracer derived from unaffected individuals is catabolized faster in homozygous and heterozygous Tangier subjects compared with normal controls (20, 21). The hypercatabolism might not be explained by a chronic decrease in HDL pool size, because acute repletion of the HDL pool by acute infusion of HDL to bring the plasma HDL concentration to a normal range did not ameliorate the hypercatabolism of HDL particles (22). One possible explanation for the increased HDL catabolism in Tangier subjects is that spherical plasma HDL particles fail to obtain lipid by ABCA1-mediated efflux, resulting in smaller particle size and more rapid catabolism (23), although this hypothesis alone would not account for the increased catabolism observed when mature, large HDL particles are infused in subjects with Tangier disease. However, in support of this hypothesis, heterozygous Tangier subjects have HDL concentrations that are 50% of normal, but the decrease in concentration is selective for the largest α-migrating subfractions (23, 24). Overexpression of ABCA1 in mice results in increases in HDL size as well as HDL concentration (25–27). One possible interpretation of these data is the direct input of FC and PL into large HDL particles by ABCA1. However, data supporting a role for ABCA1 in exporting cellular lipid to HDL particles are conflicting; studies using cells transfected with *ABCA1* have shown minimal lipid efflux to plasma HDL (28), whereas fibroblasts from Tangier patients have diminished lipid efflux to HDL compared with fibroblasts from unaffected relatives (29, 30). In a homozygous Tangier patient, the larger HDL subfractions (HDL_{2b} and HDL_{2a}) disappeared from plasma faster after HDL infusion than did the smaller HDL particles (HDL_3) (22). These data together suggest a role for ABCA1 in HDL subfraction catabolism in vivo that is not well understood.

The purpose of the present study was to determine the relationship between ABCA1 expression and in vivo HDL catabolism, including intravascular remodeling, plasma clearance, and tissue uptake of HDL. We performed our study using mice with zero, one, or two active *Abca1* alleles and expressing the human apoA-I transgene, which is necessary for mice to exhibit plasma HDL size heterogeneity similar to that observed in humans (31, 32). Human apolipoprotein A-I transgenic (*hA-I*^{Tg}) mice have been used previously to study HDL subfraction metabolism (33). The results show that ABCA1 is not necessary for the remodeling of small HDLs to larger HDL particles, but PLTP and HL are, and that plasma HDL particles are hypercatabolized selectively by the kidney, but not the liver, in *Abca1*$^{-/-}$ mice compared with wild-type controls.

EXPERIMENTAL PROCEDURES

Generation of *Abca1*$^{-/-}$ mice

A 1.65 kb PCR-generated fragment containing *Abca1* exon 16 (short arm) was inserted between the PGK terminator of the PGKNeo cassette and the double PGKtk cassettes of pPN2T (34) at *Eco*RI and *Bam*HI sites. A 12 kb fragment from intron 22 to exon 30 (long arm) was generated using the TaqPlus Long PCR System (Stratagene, La Jolla, CA) and then inserted on the PGK promoter side of the PGKNeo cassette at blunted *Xho*I and *Not*I sites to generate the final targeting vector pAbc1SALA. The composition of the knockout vector is shown in **Fig. 1A**.

Embryonic stem cells (ESVJ ES) from Genome Systems (St. Louis, MO) were electroporated by the *Not*I linearized targeting vector pAbc1SALA and screened by sequential selection with G418 and fialuridine. Embryonic stem cell colonies were screened for the targeting event by PCR using a forward primer (I15.fwd, 5′-CAAATCCCTGACCAGGACAT-3′) lying in intron 15, 83 bp 5′ of the 1.65 kb region of homology, and a reverse primer (N1, 5′-GCCTTCTTGACGAGTTCTTCTG-3′) located within the PGKNeo cassette. Targeting in PCR-positive clones was confirmed by Southern blot analysis (*Bam*HI-digested genomic DNA) with probe I14, a 381 bp fragment generated from intron 14. Primers for probe I14 were I14.fwd (5′-GCCTGGTTCAGTGTCCACAG-3′) and I14.rev (5′-TGATGAGGACATGAAGCCCAT-3′). Genomic DNA bands from the wild-type allele and the deletion allele were 6,648 and 2,922 bp, respectively. Correctly targeted embryonic stem cell clones were used to generate chimeric mice using standard procedures (35). Chimeric males were bred with C57BL/6J animals (Charles River Laboratories, Wilmington, MA) to create mice heterozygous for the targeted allele on the 129Sv/C57 mixed background. These heterozygotes were intercrossed to produce the wild-type, heterozygote, and homozygote littermates. Genotyping of mice was performed by PCR using the following primers: I16.fwd, 5′-GGAGTTGTTGGAAAGCTGTGG-3′ (located in intron 16 of the 1.65 kb region of homology); I17.rev, 5′-GAGCCAGATAGGGTTCCCTTAA-3′ (located in intron 17 within the 5.7 kb region deleted by the targeting event); and N1 primer (see above). The size of the PCR product from I16.fwd/I17.rev was 503 bp for the wild type, and that from I16.fwd/N1 was 618 bp for the deleted allele.

Abca1 knockout mice were crossed with *hA-I*^{Tg} mice (line 427) from Charles River Laboratories to generate *hA-I*^{Tg} Abca1$^{+/+}$ (wild type), *hA-I*^{Tg} Abca1$^{+/-}$ (heterozygous), and *hA-I*^{Tg} Abca1$^{-/-}$ (homozygous) mice. The mice were housed in the Wake Forest University School of Medicine transgenic facility and maintained on a chow diet. All protocols and procedures were approved by the Animal Care and Use Committee of the Wake Forest University School of Medicine.

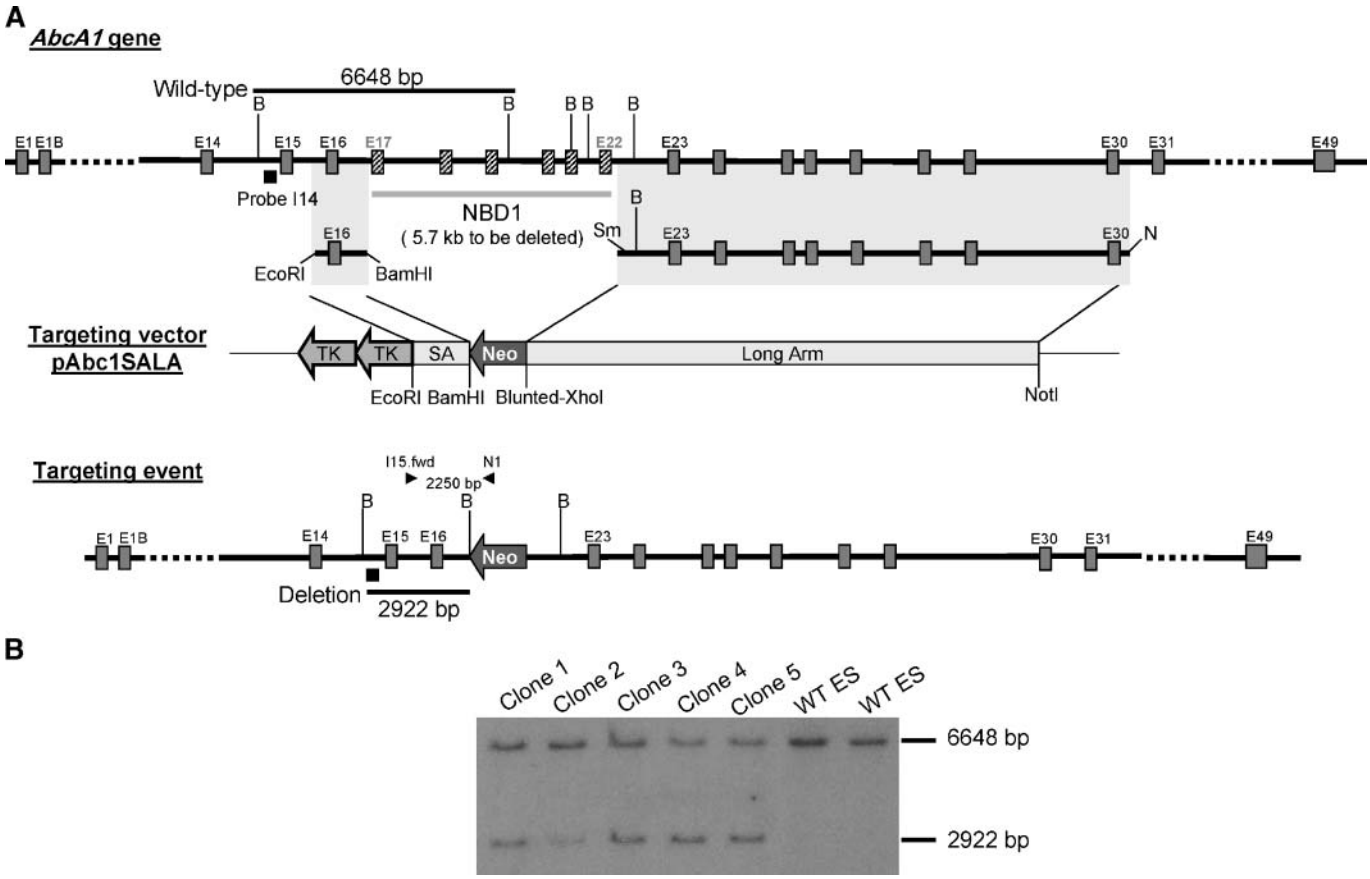

Fig. 1. Gene-targeting strategy for the mouse *AbcA1* gene. A: Strategy for disruption of the mouse *Abca1* gene. The map of the endogenous mouse *Abca1* gene is shown in the top panel. The targeting vector pAbc1SALA (middle panel) was designed to delete exons 17–22, which encode the first nucleotide binding domain (NBD1). The bottom panel represents the targeted allele after homologous recombination, in which the PGKNeo gene has replaced exons 17–22 of the mouse *Abca1* gene. B: Southern blot analysis of the targeting event. Embryonic stem (ES) cells were subjected to Southern blot analysis to screen the targeted embryonic stem cells. Positive clones (clones 1–5) have *Bam*HI-digested genomic DNA bands at 6.6 and 2.9 kb from wild-type and targeted alleles, respectively, and wild-type (WT) embryonic stem cells have a single band at 6.6 kb.

Plasma lipid, lipoprotein, and apolipoprotein analyses

Plasma total cholesterol, FC, and PL concentrations were determined by enzymatic analysis (Wako Chemicals) (36). Esterified cholesterol (EC) concentration was calculated by subtracting FC from total cholesterol concentration. HDL cholesterol was measured by enzymatic assay in the supernatant of plasma after precipitation of apoB-containing lipoproteins with heparin-manganese. Plasma human or mouse apoA-I concentrations in plasma were quantified by ELISA using monospecific antiserum to monkey or antibody to mouse apoA-I (Biodesign, Saco, MA), respectively (37). The assays were standardized with purified human or mouse apoA-I.

Plasma lipoprotein distribution was determined by fast-protein liquid chromatography (FPLC). Pooled mouse plasma (100 μl) from each genotype of mice was applied to two Superose 6 (1 × 30 cm) columns in series, and total cholesterol concentration in 100 μl of each fraction was measured by enzymatic assay to obtain the lipoprotein elution profile.

Two-dimensional gel electrophoresis was also performed to separate plasma lipoproteins by charge and size. In the first dimension, 1 μl of plasma was separated on 0.5% agarose gels (Paragon Lipo gels; Beckman Coulter, Fullerton, CA) at 100 V for 1 h. Each lane of the agarose gel was cut and laid on top of a 4–30% nondenaturing gradient gel (38) for second dimensional electrophoresis at 1,400 V/h at 10°C. Lipoproteins were then transferred to polyvinylidene difluoride membranes (Millipore), and human apoA-I distribution was determined by immunoblot analysis using goat anti-human apoA-I antibody (Biodesign) and ^{125}I-radiolabeled anti-goat IgG for visualization of human apoA-I by PhosphorImager analysis.

Plasma LCAT, PLTP, and HL activities

Exogenous LCAT activity in plasma was determined as described previously (39). Recombinant HDL particles containing 1-palmitoyl-2-oleoyl-*sn*-glycero-3-phosphocholine, [^{3}H]cholesterol, and human apoA-I were synthesized using a cholate dialysis method and used as substrates to measure plasma LCAT activity (40). Five microliters of plasma were incubated with a saturating substrate concentration of recombinant HDL cholesterol (3 μM) for 2 h at 37°C, after which conversion of radiolabeled FC to EC was determined (39).

PLTP activity was measured with a commercially available fluorescent assay kit (Cardiovascular Target, New York, NY) according to the manufacturer's instructions. Three microliters of plasma were incubated with donor and acceptor liposomes for 15 min at 37°C, and the florescence intensity increase, indicative of the transfer of quenched fluorescent PL in donor liposomes to acceptor liposomes, was measured at an excitation wavelength of 465 nm and an emission wavelength of 535 nm.

HL activity in plasma was determined using Triton X-100-stabilized triolein as substrate (41). Thirty microcuries of glycerol tri[9,10(n)-^{3}H]oleate (10–30 Ci/mmol; Amersham) and 230 μl of unlabeled triolein (200 mg/ml in $CHCl_3$) were dried under N_2, and subsequently, 1.13 ml of 1 M Tris-HCl (pH 8.6), 0.95 ml of 1% Triton X-100, and 5 ml of water were added to the dried substrate. After four 1 min sonication periods, punctuated with 1 min incubations on ice, 1.18 ml of 20% fatty acid free-BSA (in TBS, pH 8), 0.29 ml of 4 M NaCl, and 3 ml of water were added, and the final substrate solution was mixed well. Plasma HL activity was measured by incubating 20 μl of plasma (source of enzyme), 265 μl of substrate, and 95 μl of 4 M NaCl (to inhibit lipoprotein lipase activity) for 30 min at 37°C. The reactions were stopped by adding 3.25 ml of $CHCl_3$/methanol/heptane (1.37:1.28:1). Then, 1 ml of K_2CO_3 (adjusted to pH 10.5 with saturated boric acid) was added to the stopped reaction, the phases were separated by centrifugation at 1,500 *g* for 20 min, and free fatty acid released was determined by ^{3}H radiolabel quantification in 1 ml of the aqueous phase.

Membrane isolation and Western blot analysis of ABCA1 in the liver

Mouse liver samples (~500 mg) were homogenized with a Teflon homogenizer in isolation buffer (250 mM sucrose and 10 mM triethanolamine HCl, pH 7.6) containing protease inhibitors (0.1 mM PMSF in 95% ethanol, 10 μg/ml pepstatin, 10 μg/ml leupeptin, and 10 μg/ml aprotinin) for a final concentration of 10% (w/v). Homogenized tissues were centrifuged for 10 min at 3,300 *g* at 4°C to pellet cell debris and nuclei. The supernatant was recovered and centrifuged again for 20 min at 27,000 *g* at 4°C, and the recovered pellet was washed two times by resuspension in the original volume of isolation buffer followed by centrifugation for 20 min at 27,000 *g* at 4°C. After the final resuspension of pellet in isolation buffer, protein concentration was determined using the Protein BCA Assay (Pierce).

Western blot analysis was performed with 100 μg of isolated liver membrane protein. Samples were incubated at 37°C for 30 min in SDS-PAGE sample buffer and subjected to 4–16% SDS-PAGE. Proteins were transferred to nitrocellulose membranes (Schleicher and Schuell), and immunodetection was performed for ABCA1 using a polyclonal antibody, raised to a 24-mer peptide of the C-terminal region of mouse ABCA1, or for β-actin (Sigma) as a load control.

ABCA1 and β-actin signals were visualized using ^{125}I-radiolabeled secondary antibody and quantified by PhosphorImager analysis. ABCA1 protein expression was normalized to β-actin for each sample.

Isolation and iodination of small HDLs

HDL particles were isolated from *hA-I^{Tg}* mouse plasma using anti-human apoA-I immunoaffinity chromatography to avoid the potential for HDL subfraction modification induced by ultracentrifugation (42–44) and radiolabeled with ^{125}I-labeled tyramine cellobiose (TC) as described previously (33). Subsequently, ^{125}I-TC-radiolabeled HDL particles were fractionated by size-exclusion chromatography using three Superdex 200 HR FPLC columns (Amersham Biosciences) in series, after which individual fractions were run on a 4–30% nondenaturing gradient gel at 1,400 V/h at 10°C, and the gels were developed using PhosphorImager analysis (33). Fractions were pooled to give homogenous small (7.2–8.2 nm diameter) HDL particles. Small HDL tracer particles were characterized as described previously (33). The specific activity of the tracers ranged from 38 to 450 cpm/ng protein, and TCA-precipitable radioactivity was >98%.

In vivo kinetic study

In vivo kinetic study was performed with ^{125}I-radiolabeled small HDL particles as described previously (33). Briefly, 1.5–3.0 × 10^5 cpm of the radiolabeled tracer was injected into the jugular vein of anesthetized recipient *hA-I^{Tg}* ABCA1$^{+/+}$, *hA-I^{Tg}* ABCA1$^{+/-}$, and *hA-I^{Tg}* ABCA1$^{-/-}$ mice. Blood samples were obtained by retro-orbital bleeding at 5, 10, 20, and 30 min and at 1, 2, 3, 5, 8, and 24 h after dose injection. Aliquots of plasma from the various time points were fractionated on 4–30% nondenaturing gradient gels at 1,400 V/h at 10°C to determine the fractional distribution of apoA-I radioactivity. After electrophoresis, gels were exposed in a PhosphorImager cassette and the images were developed and quantified using a Typhoon 8600 (Molecular Dynamics, Sunnyvale, CA) and ImageQuant software (version 5.2). In the analysis, regions corresponding to pre-β (<7.2 nm), small (7.2–8.2 nm), and medium (8.2–10.4 nm) HDLs were quantified. Twenty-four hours after dose injection, animals were killed, tissues were harvested and digested with 1 N NaOH overnight at 60°C, and an aliquot of the digest was taken for ^{125}I radiolabel quantification. The fractional catabolic rate (FCR) values for HDL tracer decay from whole plasma and uptake by tissues were determined using SAAM (Simulation, Analysis, and Modeling) software as described previously (33).

In vitro incubation study

Plasma samples (20 μl) obtained from *hA-I^{Tg}* ABCA1$^{+/+}$, *hA-I^{Tg}* ABCA1$^{-/-}$, *hA-I^{Tg}* HL$^{-/-}$, *PLTP$^{+/+}$*, *PLTP$^{-/-}$*, *LCAT$^{+/+}$*, and *LCAT$^{-/-}$* mice were incubated with ^{125}I-TC-radiolabeled small HDLs (20,000 cpm) at 37°C for 5 or 60 min. Subsequently, plasma samples were subjected to 4–30% nondenaturing gradient gel electrophoretic separation and PhosphorImager analysis.

For the chemical inhibition study, plasma samples from *hA-I^{Tg}* ABCA1$^{+/+}$ and *hA-I^{Tg}* ABCA1$^{-/-}$ mice were preincubated in the absence or presence of DTNB (5 mM final concentration) or PMSF (10 mM final concentration) at 37°C for 30 min to inhibit LCAT or HL, respectively. After the 30 min incubation, ^{125}I-TC-radiolabeled small HDL particles were added to plasma and subsequently incubated at 37°C for 5 and 60 min, after which the plasma samples were analyzed as described above. To quantify the degree of inhibition of LCAT and HL, plasma samples preincubated with and without either inhibitor were assayed for LCAT and HL activities, as described above.

Statistical analysis

The results are expressed as means ± SD. Differences among the genotypes of mice were analyzed using one-way ANOVA, followed by Tukey's multiple comparison test to identify individual differences. All statistical analyses were performed using the InStat program (GraphPad Software, Inc., San Diego, CA).

RESULTS

Plasma lipid and lipoprotein analysis of *hA-I^{Tg} Abca1* knockout mice

Elimination of ABCA1 function was accomplished by targeted deletion of exons 17–22, which encode the first nucleotide binding domain of ABCA1 (Fig. 1A). Embryonic stem cells were electroporated with the linearized targeting construct, and those that survived positive and negative selection were verified as correctly targeted by Southern blot analysis (2.9 kb band in clones 1–5; Fig. 1B). *Abca1* knockout mice and littermate controls were generated and crossed with *hA-I^{Tg}* mice to generate the mice used for this study.

Table 1 shows a summary of plasma measurements made on the mice. Compared with *hA-I^{Tg}* ABCA1$^{+/+}$

TABLE 1. Plasma measurements of *hA-I*^{Tg} Abca1 knockout mice

Genotype	Total Plasma Cholesterol	HDL Cholesterol	Free Cholesterol	Esterified Cholesterol	Phospholipid	hApoA-I	mApoA-I	LCAT	HL	Phospholipid Transfer Protein
					mg/dl					
hA-I^{Tg} *Abca1*$^{+/+}$	210 ± 55^{a} (21)	189 ± 29^{a} (5)	83 ± 22^{a} (11)	121 ± 37^{a} (11)	426 ± 47^{a} (10)	296 ± 84^{a} (12)	26 ± 9^{a} (4)	54 ± 4^{a} (7)	9 ± 0.5^{a} (5)	10,238 ± 4,139^{a} (10)
hA-I^{Tg} Abca1$^{+/-}$	130 ± 43^{b} (20)	104 ± 27^{b} (4)	52 ± 30^{b} (13)	62 ± 16^{b} (13)	319 ± 68^{b} (9)	248 ± 127^{a} (13)	17 ± 15^{ab} (5)	50 ± 6^{a} (7)	8 ± 2^{a} (5)	11,856 ± 6,279^{a} (9)
hA-I^{Tg} *Abca1*$^{-/-}$	35 ± 20^{c} (16)	28 ± 13^{c} (3)	7 ± 9^{c} (7)	23 ± 13^{c} (7)	100 ± 32^{c} (9)	5 ± 5^{b} (3)	0.6 ± 0.1^{b} (3)	30 ± 14^{b} (7)	5 ± 0.3^{b} (5)	917 ± 853^{b} (8)

hA-I^{Tg}, human apolipoprotein A-I transgenic; hApoA-I, human apolipoprotein A-I; mApoA-I, mouse apoA-I. Data represent means ± SD. Number of mice is given in parentheses. Values in each column with different superscript letters are significantly different from each other at $P < 0.05$. Activity units are as follows: nmol cholesteryl ester formed/h/ml plasma for LCAT, μmol FA released/h/ml plasma for HL, and arbitrary units for PLTP.

mice, plasma total cholesterol, FC, EC, HDL cholesterol, and PL concentrations were significantly lower in *hA-I*^{Tg} ABCA1$^{-/-}$ mice, and all values in *hA-I*^{Tg} ABCA1$^{+/-}$ mice were intermediate, indicating a gene-dosage-related response. The gene-dosage-related trends for plasma lipid and apoA-I concentrations were similar to those observed for other *Abca1* knockout mice (45, 46), except that our values were higher for each *Abca1* genotype. This result demonstrates that low HDL concentrations that result from inactive ABCA1 can be compensated to some degree by transgenic overexpression of human apoA-I. For instance, HDL cholesterol concentrations ranged from 41 to 57 mg/dl in *Abca1*$^{+/-}$ mice in the absence of *hA-I*^{Tg} overexpression (45, 46) but were 104 mg/dl in mice expressing the human transgene. In addition, HDL cholesterol and plasma FC and EC concentrations in heterozygotes were 50–60% of wild-type values, as anticipated, but PL and human apoA-I concentrations were 75–84% of normal, suggesting partial compensation of plasma PL and apoA-I concentrations for the loss of one active *Abca1* allele by transgenic overexpression of human apoA-I.

We determined the activity of several proteins known to be important in the remodeling and metabolism of HDL subfractions. Plasma LCAT activity in *hA-I*^{Tg} ABCA1$^{-/-}$ mice was half that of wild-type or heterozygous knockout mice (Table 1), consistent with the finding that a Tangier patient had lower than normal LCAT activity (47). Likewise, similar activities for HL and PLTP were observed for wild-type and heterozygous knockout mice, but significantly lower activity was observed for both proteins in *hA-I*^{Tg} ABCA1$^{-/-}$ mice; this was particularly apparent for PLTP activity, which was 9% of that measured in *hA-I*^{Tg} wild-type mice.

Plasma samples from each genotype of mice were further analyzed by FPLC and two-dimensional gel electrophoresis. Consistent with the results obtained by measurement of plasma HDL cholesterol concentration by heparin-manganese precipitation, FPLC analysis confirmed reduced HDL cholesterol in heterozygous knockout mice and nearly absent HDL cholesterol in *hA-I*^{Tg} ABCA1$^{-/-}$ mice (**Fig. 2A**). In addition, the HDL cholesterol elution profile of *hA-I*^{Tg} ABCA1$^{+/-}$ mice was shifted to longer elution times, suggesting small average HDL particle size in these animals (Fig. 2A). Two-dimensional gel electrophoresis of plasma followed by immunoblot analysis with anti-human apoA-I antibody was used to observe HDL particle size and charge heterogeneity. Nontransgenic mice have a single, apparently homogeneous HDL particle ~10 nm in diameter; however, overexpression of *hA-I*^{Tg} resulted in heterogeneous subfractions of HDL similar to those observed in human plasma (31, 32). Using this system, we found qualitatively similar patterns of HDL subfractions in our wild-type and heterozygous knockout mice, with a suggestion of a slight reduction in the amount of small HDL particles (7.2–8.2 nm) in the heterozygotes (Fig. 2B). Note that the amount of apoA-I distributed in medium (8.2–10.4 nm) and large (10.4–12.2 nm) HDL particles of *hA-I*^{Tg} ABCA1$^{+/-}$ mice was only slightly less than that of *hA-I*^{Tg} mice, suggesting that *hA-I*^{Tg} ABCA1$^{+/-}$ mice have fewer large and medium HDL particles in plasma, at least based on cholesterol content (Fig. 2A), that are enriched in apoA-I relative to the small HDL particles (Fig. 2B). Finally, under our experimental conditions, we could not detect any human apoA-I in the plasma of *hA-I*^{Tg} ABCA1$^{-/-}$ mice.

Hepatic ABCA1 protein expression in *hA-I*^{Tg} mice

One of the intriguing findings in the plasma lipid measurements was a lower HDL cholesterol concentration in heterozygous compared with wild-type mice, with little change in plasma apoA-I concentrations (Table 1). Results from in vitro studies have shown that interaction of apoA-I with ABCA1 stabilizes ABCA1 protein, protecting it from degradation by calpain protease (48, 49). However, this has never been demonstrated in vivo. On the basis of the in vitro data and our higher than expected apoA-I concentrations in the plasma of heterozygous knockout mice, we explored the possibility that transgenic overexpression of human apoA-I may stabilize ABCA1 protein, resulting in increased ABCA1 protein expression and maintenance of plasma apoA-I levels. Because hepatic ABCA1 has been shown to be responsible for maintaining 80% of the plasma HDL pool in chow-fed mice (50), we explored this hypothesis by analyzing hepatic ABCA1 protein expression in wild-type and *ABCA1*$^{+/-}$ mice with and without *hA-I*^{Tg} expression. Western blot analysis of hepatic membranes from *hA-I*^{Tg} mice demonstrated a 2-fold increase in ABCA1 protein expression (*hA-I*^{Tg} ABCA1$^{+/+}$ = 1.06 ± 0.51) compared with nontransgenic controls (*ABCA1*$^{+/+}$ = 0.45 ± 0.16; **Fig. 3**). As expected, hepatic

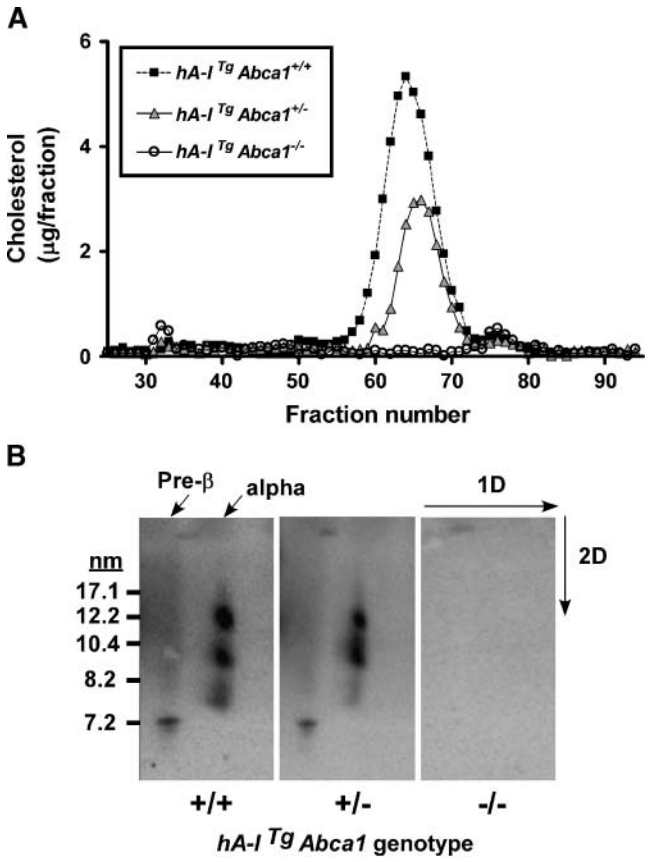

Fig. 2. Plasma lipoprotein analysis of human apolipoprotein A-I transgenic (*hA-I*^{Tg}) *Abca1* knockout mice. A: Fast-protein liquid chromatography (FPLC) cholesterol elution profile of plasma from chow-fed mice of the indicated genotype. One hundred microliters of pooled mouse plasma were fractionated by FPLC, and the cholesterol concentration of each fraction was determined by enzymatic assay. B: Western blot analysis for human apolipoprotein A-I (apoA-I) in plasma. One microliter of mouse plasma from each indicated genotype was separated on a 0.5% agarose gel (first dimension; 1D) and subsequently by 4–30% nondenaturing gradient gel electrophoresis (second dimension; 2D). After two-dimensional gel electrophoresis, the proteins were transferred to nitrocellulose and the blot was incubated with anti-human apoA-I antiserum. The blot was visualized using ^{125}I-radiolabeled secondary antibody and PhosphorImager analysis.

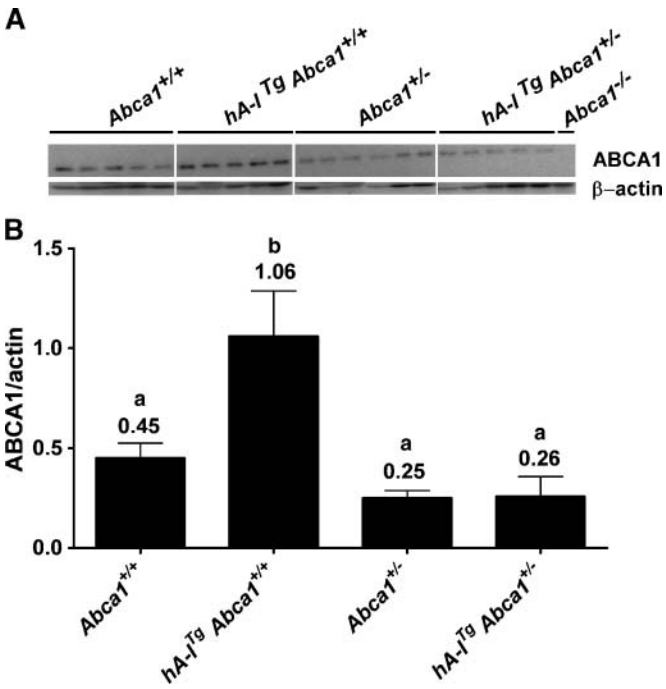

Fig. 3. Effect of *hA-I*^{Tg} expression on hepatic ABCA1 protein in wild-type and heterozygous *Abca1* knockout mice. A: Liver membranes were isolated from mice of the indicated genotypes, and proteins were fractionated by SDS-PAGE. After electrophoretic transfer of the proteins to nitrocellulose, the blot was probed with anti-human ABCA1 antiserum or with anti-mouse β-actin antiserum. The blot was developed with a ^{125}I-radiolabeled secondary antibody and PhosphorImager analysis. PhosphorImager results for five to six individual mice of each genotype are shown; liver membrane protein from an *Abca1*$^{-/-}$ mouse is also shown as a negative control (far right lane). B: The PhosphorImager results are quantified as the ratio of ABCA1/β-actin (means ± SD). Values with unlike letters are significantly different by ANOVA ($P < 0.001$) and Tukey's posthoc analysis. Using an unpaired *t*-test, ABCA1 protein expression was significantly different ($P = 0.04$) for liver membranes from *Abca1*$^{+/+}$ versus *Abca1*$^{+/-}$ mice.

ABCA1 protein expression in *Abca1*$^{+/-}$ mice was half that of wild-type mice (0.25 ± 0.09 vs. 0.45 ± 0.16, respectively). Surprisingly, overexpression of *hA-I*^{Tg} had no effect on ABCA1 protein expression in mice heterozygous for the *Abca1* gene (0.26 ± 0.22 vs. 0.25 ± 0.09), suggesting that the stabilization of hepatic ABCA1 protein by overexpression of human apoA-I requires two active alleles of the *Abca1* gene. Hepatic mRNA for *Abca1* was similar among the four genotypes of mice (data not shown), suggesting that differences in *Abca1* gene transcription could not account for the observed difference in hepatic ABCA1 protein.

Plasma turnover and tissue uptake of small HDL tracer particles

To perform an in vivo kinetic study, homogenous small HDL particles were isolated using anti-human apoA-I immunoaffinity and size-exclusion chromatography to prevent structural alterations in HDL particles induced by ultracentrifugation (42–44) and were radiolabeled with ^{125}I-TC. The small HDL tracer particles were relatively homogenous in size (7.2–7.7 nm diameter; **Fig. 4A**), and >85% of the radiolabel was associated with monomeric apoA-I (28 kDa), determined by PhosphorImager analysis of SDS 4–16% gradient polyacrylamide gels (Fig. 4B). The bands larger than 67 kDa in Fig. 4B were immunoreactive with antibody against human apoA-I, suggesting that they may be oligomers of apoA-I formed during the TC radiolabeling of HDL particles.

^{125}I-TC-radiolabeled small HDL tracer was injected into recipient mice, and the turnover of the tracer in plasma was monitored for 24 h before the animals were killed and tissues were harvested. The injected mass of apoA-I in the HDL tracer was <7% of the plasma apoA-I pool for all recipient mice. Whole plasma die-away of small HDL tracer was significantly faster in *hA-I*^{Tg} Abca1$^{-/-}$ recipient mice (3.84 ± 0.64 pools/day) compared with wild-type mice (2.35 ± 0.35 pools/day) and heterozygous knockout re-

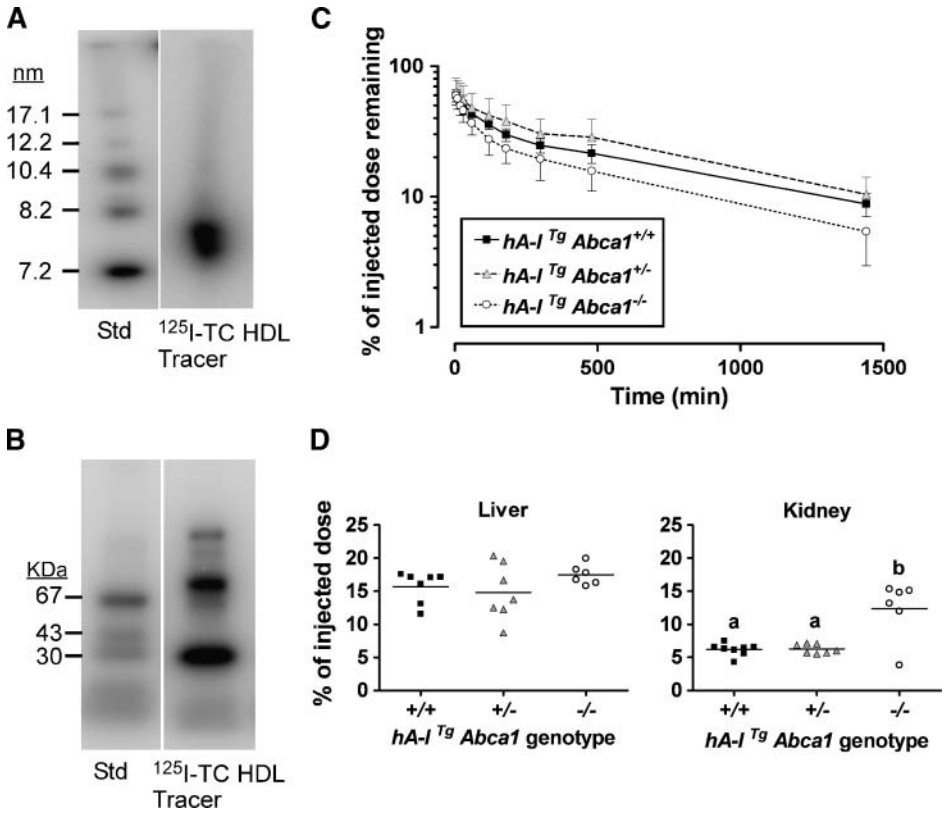

Fig. 4. In vivo catabolism and tissue uptake of small HDL tracer in *hA-I*^{Tg} Abca1 knockout recipient mice. A: PhosphorImager analysis of ^{125}I-labeled tyramine cellobiose (TC)-radiolabeled small HDL tracer separated on a 4–30% nondenaturing gradient gel (1,400 V/h at 10°C). Stokes' diameters of high molecular mass standard proteins are shown at left for reference. B: PhosphorImager analysis of a 4–16% polyacrylamide SDS gel of ^{125}I-TC small HDL tracer. Molecular masses of standard proteins are shown at left. C: Whole plasma decay of small HDL tracer in recipient mice of the indicated genotype. Radioactivity in plasma at each time point was quantified and converted to percentage of injected radioactivity remaining at the indicated times. Plasma volume was calculated as 3.5% of body weight. Values shown are means ± SD. D: Liver and kidney uptake of small HDL tracer 24 h after injection into mice of the indicated genotype. Liver and kidney samples were digested overnight in 1 N NaOH at 60°C, and ^{125}I radioactivity was quantified. Data are expressed as percentage of injected ^{125}I-TC HDL tracer; each point represents data from an individual animal, and the horizontal line denotes the mean for each genotype. Kidney uptake values with unlike letters were significantly different ($P < 0.001$) by ANOVA and Tukey's posthoc analysis; no difference was observed among genotypes for liver uptake.

cipient mice (2.09 ± 0.31 pools/day) (Fig. 4C, **Table 2**, whole plasma). Twenty-four hours after tracer injection, 90% of the recovered radioactivity was in the liver and kidneys (data not shown). Liver uptake of small HDL tracer was nearly 3-fold greater in wild-type mice compared with kidney uptake (Fig. 4D). However, tracer uptake by the liver was similar among the three genotypes of mice, suggesting that the absence of ABCA1 did not alter the catabolism of HDL apoA-I by the liver. In contrast, kidney uptake by *hA-I*^{Tg} Abca1$^{-/-}$ recipient mice was 2-fold ($P < 0.001$) greater than that in wild-type and heterozygous knockout mice. The liver FCR of the tracer, which is calculated as the product of plasma FCR and liver uptake of tracer, was 40% higher ($P < 0.05$) in the homozygous knockout mice compared with wild-type and heterozygous mice as a result of the higher plasma FCR in the former. Together, these results suggest that the higher uptake of HDL tracer by the kidney in *hA-I*^{Tg} Abca1$^{-/-}$ mice was not the result of increased nonspecific uptake by all tissues caused by the very low HDL pool size in these recipient mice (Table 1), because liver uptake was higher than kidney uptake and not different among genotypes.

In vivo remodeling of small HDL tracer particles in *hA-I*^{Tg} *Abca1* knockout mice

Plasma samples taken during the 24 h turnover study were subjected to nondenaturing gradient gel electrophoresis followed by PhosphorImager analysis to monitor in vivo remodeling of the small HDL tracer during the turnover study. **Figure 5** shows PhosphorImager analysis of gels from three representative *hA-I*^{Tg} Abca1$^{+/+}$ and *hA-I*^{Tg} Abca1$^{-/-}$ recipient mice. Within 5 min after the tracer injection, most of the injected small HDL tracer was remodeled to medium-sized (~8.2 nm diameter) HDLs in *hA-I*^{Tg} Abca1$^{+/+}$ and *hA-I*^{Tg} Abca1$^{+/-}$ mice (data not shown). Remodeling of the tracer to medium-sized HDLs also oc-

TABLE 2. Plasma and tissue FCRs of small HDL tracer

Genotype	Whole Plasma	Subfractionated Plasma			Tissue	
		Pre-β	Small	Medium	Liver	Kidney
hA-I^{Tg} *Abca1*$^{+/+}$	2.35 ± 0.35^{b}	3.08 ± 1.43^{b}	4.03 ± 1.96	1.72 ± 0.52^{b}	0.85 ± 0.07^{b}	0.34 ± 0.04^{b}
hA-I^{Tg} *Abca1*$^{+/-}$	2.09 ± 0.31^{b}	2.26 ± 1.08^{b}	3.09 ± 1.49	1.81 ± 0.40^{b}	0.60 ± 0.07^{c}	0.27 ± 0.07^{b}
hA-I^{Tg} *Abca1*$^{-/-}$	3.84 ± 0.64^{a}	5.51 ± 0.72^{a}	4.49 ± 1.68	3.97 ± 0.70^{a}	1.19 ± 0.26^{a}	0.88 ± 0.36^{a}

Fractional catabolic rates (FCRs) are expressed as pools/day. Values were calculated using SAAM (Simulation, Analysis, and Modeling) software and a two-pool model with rate constants from the plasma pool to the liver and kidney. FCR values for subfractionated HDL were determined by 4–30% nondenaturing gradient gel electrophoresis of plasma samples at each time point after dose injection; subsequently, PhosphorImager analysis was conducted to quantify radiolabel distribution in the pre-β, small, and medium regions of each lane, which were converted into a fractional distribution. The fractional distribution was then multiplied by the cpm/ml plasma for each time point to obtain cpm/ml for each HDL subfraction region, and the values were used for kinetic modeling. Data represent means ± SD (n = 6–8). Statistical analyses of FCR values among the three genotypes were performed using one-way ANOVA with Tukey's multiple comparison test to ascertain individual differences. Values in each column with different superscript letters are significantly different from each other at $P < 0.05$.

curred in *hA-I*^{Tg} Abca1$^{-/-}$ recipient mice, but unlike the results from wild-type and heterozygous knockout recipient mice, there was detectable radiolabel in the pre-β size range of the gel (~7.2 nm) for three of six recipient mice. This result suggests that active ABCA1 protein was not necessary for the remodeling of small HDLs to medium-sized HDL particles. FCR values for each HDL subfraction, determined by kinetic analysis of the PhosphorImager data, are shown in Table 2. Consistent with the whole plasma FCR data for small HDL tracer, *hA-I*^{Tg} Abca1$^{-/-}$ recipient mice displayed significantly faster clearance of pre-β and medium HDLs from the plasma than did wild-type and heterozygous knockout mice.

In vitro remodeling of small HDL tracer in the plasma of *hA-I*^{Tg} *Abca1* knockout mice

In vitro incubation of mouse plasma with small HDL tracer was performed to determine which plasma factors are necessary to promote the HDL remodeling observed in vivo. Plasma proteins, such as PLTP (51–53), HL (54), and LCAT, have been implicated in HDL remodeling and were investigated using genetic disruption and chemical inhibition of activity. Plasma samples from *hA-I*^{Tg} HL$^{-/-}$, *PLTP*$^{-/-}$, and *LCAT*$^{-/-}$ mice and their respective wild-type controls were incubated with small HDL tracer for 5 or 60 min, and remodeling was detected by nondenaturing gradient gel electrophoresis and PhosphorImager

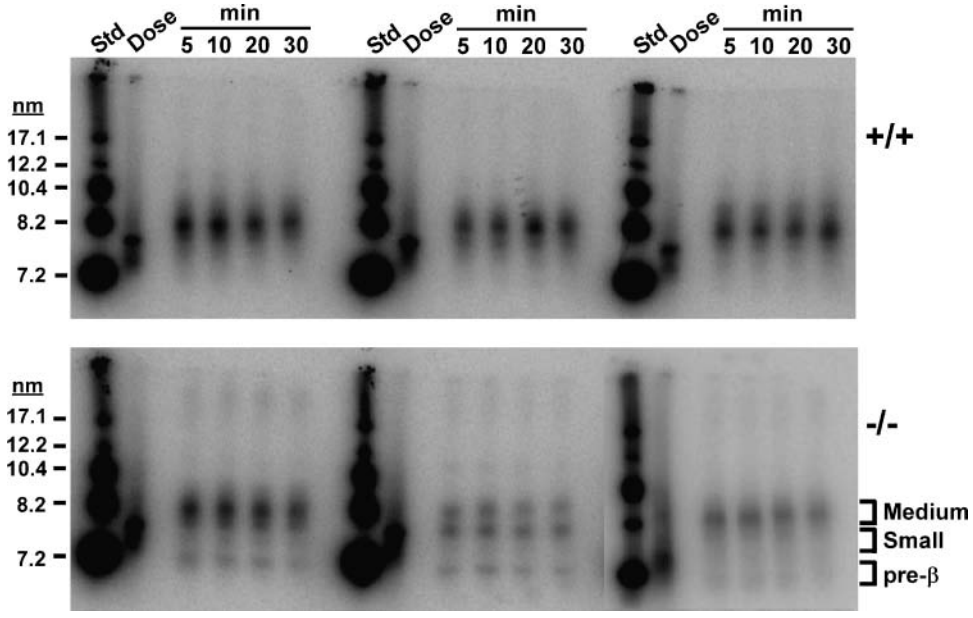

Fig. 5. In vivo remodeling of small HDL tracer after intravenous injection into *hA-I*^{Tg} Abca1$^{+/+}$ and *hA-I*^{Tg} Abca1$^{-/-}$ recipient mice. Plasma samples, drawn at the indicated times after ^{125}I-TC-radiolabeled small HDL tracer injection, were fractionated on 4–30% nondenaturing gradient gels at 1,400 V/h at 10°C. The radiolabel distribution on gels was visualized using a PhosphorImager, and the results for three representative *hA-I*^{Tg} Abca1$^{+/+}$ (top; +/+) and *hA-I*^{Tg} Abca1$^{-/-}$ (bottom; −/−) recipient mice are shown. High molecular mass protein standard (Std) and dose are shown for reference, as are the size ranges corresponding to pre-β, small, and medium HDL particles.

analysis (**Fig. 6**). Chemical inhibitors also were used to inhibit LCAT and HL activities in the plasma of *hA-I*^{Tg} Abca1$^{+/+}$ and *hA-I*^{Tg} Abca1$^{-/-}$ mice. Inhibition of PLTP activity was not investigated, because plasma PLTP activity for *hA-I*^{Tg} Abca1$^{-/-}$ mice was 10% that of wild-type mice (Table 1).

In vitro remodeling of small HDL tracer to medium-sized HDLs was observed in the plasma of both *hA-I*^{Tg} Abca1$^{+/+}$ and *hA-I*^{Tg} Abca1$^{-/-}$ mice (Fig. 6A). This was similar to the results observed in vivo (Fig. 5) and supports the in vivo turnover data, which suggested that ABCA1 was not necessary for the remodeling of small HDLs to medium-sized particles. However, remodeling of small HDL tracer was not readily apparent in the plasma of *hA-I*^{Tg} HL$^{-/-}$ and *PLTP*$^{-/-}$ mice, suggesting a significant role of HL and PLTP in the remodeling (Fig. 6A). Some remodeling of the tracer was observed in *LCAT*$^{-/-}$ plasma, suggesting that LCAT is not required for this process (Fig. 6A).

Incubating *hA-I*^{Tg} Abca1$^{+/+}$ and *hA-I*^{Tg} Abca1$^{-/-}$ mouse plasma with DTNB at 37°C for 30 min completely inhibited LCAT activity comparable to that of LCAT knockout mice. DTNB treatment did not affect the remodeling in *hA-I*^{Tg} Abca1$^{+/+}$ mice, whereas the extent of remodeling was somewhat reduced in *hA-I*^{Tg} Abca1$^{-/-}$ mice (Fig. 6B). As *hA-I*^{Tg} Abca1$^{-/-}$ mice also have very low plasma PLTP activity, the decreased remodeling in this genotype of mice may be attributed to the near absence of both factors. PMSF is a serine-modifying reagent that can inhibit the active site serine residues of LCAT and HL. However, incubation of plasma samples with 10 mM PMSF at 37°C for 30 min did not completely inhibit LCAT and HL activities (~50% and ~20% activity of nontreated plasma, respectively), and remodeling of small HDL tracer to me-

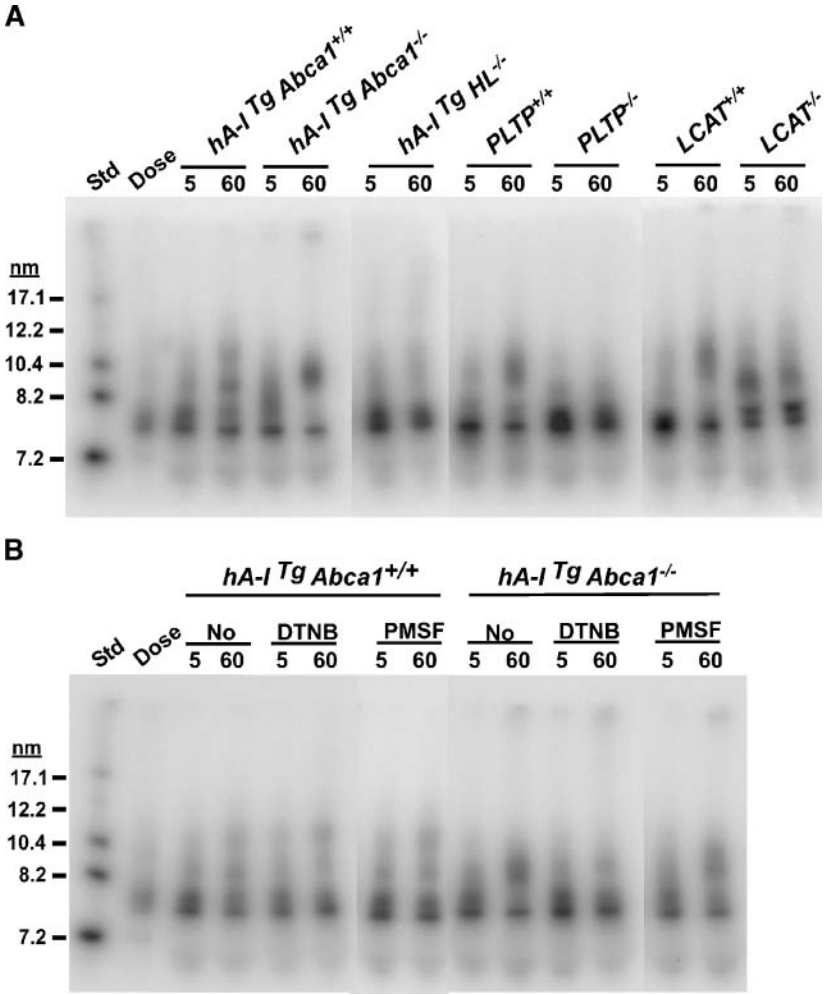

Fig. 6. In vitro incubation of small HDL tracer with mouse plasma. A: Whole plasma from *hA-I*^{Tg} Abca1$^{+/+}$, *hA-I*^{Tg} Abca1$^{-/-}$, *hA-I*^{Tg} HL$^{-/-}$, phospholipid transfer protein (*PLTP*$^{+/+}$), *PLTP*$^{-/-}$, *LCAT*$^{+/+}$, and *LCAT*$^{-/-}$ mice was incubated with ^{125}I-TC-radiolabeled small HDL tracer for 5 or 60 min at 37°C. Aliquots of incubation mixtures were subjected to 4–30% nondenaturing gradient gel electrophoresis at 1,400 V/h at 10°C. After electrophoresis, gels were developed with a PhosphorImager. High molecular mass protein standard (Std) and dose are shown for reference. B: Whole plasma samples from *hA-I*^{Tg} Abca1$^{+/+}$ and *hA-I*^{Tg} Abca1$^{-/-}$ mice were incubated with or without 5 mM DTNB or 10 mM PMSF for 30 min at 37°C. Subsequently, ^{125}I-TC-radiolabeled small HDL tracer was added to plasma samples and incubated for 5 or 60 min at 37°C. Aliquots of incubation mixtures were analyzed as described for A.

dium-sized HDLs still occurred in the plasma of both genotypes of mice. Overall, the results from the in vitro experiments suggested that PLTP and HL are required for small to medium HDL remodeling and that less than wild-type activity of each is sufficient for the process.

DISCUSSION

The purpose of this study was to investigate the role of ABCA1 in the intravascular remodeling, plasma clearance, and organ-specific uptake of HDL. Although the role of ABCA1 in the formation of nascent HDL particles is well known, its role in HDL catabolism is poorly understood. For more than two decades, it has been known that mature, spherical plasma HDL particles are hypercatabolized in subjects with Tangier disease compared with normal individuals and that the more rapid catabolism is independent of HDL pool size (20, 22). Our results contribute several novel observations that explain this finding. In mice expressing *hA-I*^{Tg}, we found a significantly faster catabolism of plasma HDL in mice lacking ABCA1 compared with mice expressing ABCA1. The 2-fold increase in plasma FCR observed in the knockout mice compared with the wild-type mice could be accounted for by a 2-fold increase in kidney catabolism of HDL apoA-I tracer with no difference in hepatic catabolism of radiolabel. This outcome demonstrates that the hypercatabolism of plasma HDL is not explained by a general increase in catabolism of HDL particles caused by reduced HDL pool size; rather, it is selectively mediated by increased kidney uptake of apoA-I, presumably as lipid-poor and/or lipid-free pre-β HDL particles. The second major finding of the study was that remodeling of small HDL tracer particles in plasma occurred in the absence of ABCA1. This observation suggests that ABCA1 functions primarily to add the requisite amount of lipid to apoA-I, forming nascent HDL particles and preventing the premature catabolism of lipid-free apoA-I by the kidney. Furthermore, ABCA1 does not appear to have a role in the maturation of small plasma HDLs to larger HDL particles. Finally, we provide the first in vivo evidence that transgenic overexpression of human apoA-I results in the expression of more hepatic ABCA1 protein, presumably by stabilizing ABCA1 and slowing its degradation, which may be an important mechanism in preventing the hypercatabolism of lipid-poor apoA-I and the increase of plasma HDL in situations in which ABCA1 interaction with apoA-I is not saturated.

Hypercatabolism of apoA-I has been observed in Tangier patients (20, 22) as well as in an animal model of ABCA1 deficiency, the Wisconsin Hypoalpha Mutant (WHAM) chicken (55, 56). However, the mechanisms responsible for the rapid catabolism of apoA-I associated with dysfunctional ABCA1 remain unknown. Initially, the mechanism was thought to be increased nonspecific catabolism of HDL by tissues attributable to the markedly reduced HDL pool size in plasma (<5% of normal). However, acute replacement of the plasma HDL pool in Tangier subjects by intravenous infusion of HDL had a minimal impact on the rapid catabolism of apoA-I tracer (22), suggesting that increased nonspecific catabolism of HDL was not a likely explanation. Studies by Schreyer, Hart, and Attie (56) demonstrated a more rapid catabolism of radiolabeled apoA-I in WHAM chickens compared with normal chickens and an increased uptake of the radiolabel by the kidney. However, whether the same mechanism applies for HDL-bound apoA-I is unknown, because only 50% of the radiolabeled apoA-I injected into WHAM chickens was bound to lipoprotein particles during the turnover study (56). A previous study has documented that apoA-I that is loosely associated with HDL is removed from the circulation more rapidly and taken up by the kidneys to a greater extent than more tightly bound HDL apoA-I (57). Most HDL tracers used for in vivo turnover studies are isolated by ultracentrifugation, which can result in particle modification (42–44) and loosely associated apoA-I. To date, no studies have addressed the tissue sites responsible for the hypercatabolism of HDL tracers in animal models of Tangier disease (i.e., WHAM chicken and *Abca1* knockout mice) using HDL tracer particles that were not subjected to ultracentrifugation. Our results are unique in this regard. Using small HDL tracer particles that had not been subjected to ultracentrifugation, we demonstrated that the uptake of radiolabeled apoA-I was 3-fold greater in liver compared with kidney in wild-type mice (Fig. 4D). In the absence of ABCA1, liver uptake of HDL apoA-I tracer was similar to that of wild-type mice; however, kidney uptake was 2-fold higher. This represents the first in vivo evidence that the hypercatabolism of plasma HDL particles in Tangier disease is likely solely the result of an increase in catabolism of apoA-I by the kidney and not of a nonspecific increase in the tissue catabolism of HDL as a result of low HDL pool size.

Previous studies in nonhuman primates suggested a unidirectional maturation pathway for plasma HDL subfractions in which small HDLs (7.2–8.1 nm), containing two molecules of apoA-I, were converted to medium (8.1–10.4 nm) or large (10.4–12.2 nm) HDLs, containing three and four molecules of apoA-I, respectively, outside the plasma compartment (14, 58). It is likely that ABCG1, and not ABCA1, is involved in the maturation of mature HDL particles outside the plasma space, because ABCG1 can transport cellular lipid to spherical HDL particles, whereas ABCA1 transports cellular lipid to lipid-free apoA-I (12, 59). A subsequent study in *hA-I*^{Tg} mice using similar experimental conditions reported that small HDL particles were remodeled rapidly in plasma to medium-sized HDLs. In the present study, we observed remodeling of small HDL tracer to medium-sized HDLs in recipient mice without active ABCA1, demonstrating that functional ABCA1 was not necessary for the remodeling (Fig. 5). Furthermore, there was no observed difference in the rate of the remodeling of small HDLs to medium HDLs or in the quantity of medium HDLs produced in the presence or absence of ABCA1, suggesting that factors in plasma may catalyze the remodeling process.

Studies have shown that PLTP can remodel HDL particles to smaller and larger HDL particles in vitro (60). HL

can reduce the size of large triglyceride-enriched HDL particles, resulting in the release of pre-β HDLs in vitro (61). LCAT is also involved in the maturation of HDL subfractions, but our previous study in *hA-I*^{Tg} mice suggested that LCAT was not necessary for the rapid remodeling we observed with our tracer particles (33). To determine whether PLTP and HL are involved in the remodeling of small HDL tracers to medium-sized HDL particles in plasma, we performed in vitro studies using plasma from mice that were deficient in PLTP and HL. Our results suggest that PLTP and HL, but not LCAT, are necessary for the remodeling, because remodeling was not apparent in plasma of *PLTP* and *HL* knockout mice (Fig. 6A). The fact that remodeling occurred in *Abca1* knockout mouse plasma, which contains 50% and 10% of wild-type HL and PLTP, respectively (Table 1), suggests that only a small amount of these plasma factors is needed to catalyze remodeling. Although the exact nature of this remodeling is unknown at present, it cannot be a random exchange of radiolabel because the tracer particles remodel to discretely sized HDL subfractions, not to all available HDL particles in plasma.

The involvement of HL in the remodeling of small HDLs to medium-sized particles seems paradoxical to its reported role in reducing the size of triglyceride-enriched HDL (61). Although we do not know the nature of this remodeling process by HL in our study, we speculate that the phospholipase A_1 activity of HL may destabilize the surface PL monolayer of HDL and facilitate the PLTP-mediated fusion of HDL particles (60). Because mouse HL normally circulates in plasma (62), it is available to modify HDL particles during in vitro incubations. It is also known that HL can stimulate the selective uptake of HDL CEs by SR-BI to a greater extent than an inactive mutant form of HL, suggesting that hydrolysis of PL by HL facilitates selective CE uptake by SR-BI to a greater extent than the ligand-bridging role of HL for HDL and SR-BI (63). In addition, transgenic overexpression of group IIa secretory phospholipase A_2 results in increased selective uptake of HDL CE by SR-BI, suggesting the HDL PL hydrolysis may destabilize the particle surface to facilitate this process (64). By analogy, if minimal hydrolysis of HDL PL destabilizes the particle surface, it may facilitate particle fusion by PLTP, resulting in the rapid remodeling of HDL particles in plasma.

ABCA1 protein expression is controlled by posttranslational as well as transcriptional mechanisms (65, 66). ABCA1 protein on the surface of cells is stabilized by the binding of apoA-I, which results in the dephosphorylation of a PEST sequence in ABCA1 and inhibits its calpain-mediated degradation (49, 67). This ABCA1 protein turnover pathway has been demonstrated in several cell types, including primary mouse hepatocytes and macrophages (49). A 2-fold increase in hepatocyte and macrophage ABCA1 protein was demonstrated in vivo after injection of a bolus of lipid-free apoA-I, which was equivalent to ~15% of the total apoA-I pool, suggesting that the stabilization by apoA-I is an important physiological mechanism to increase cell surface ABCA1 protein expression in vivo (49). However, in the same study, the authors reported that no increase in ABCA1 protein was observed in *hA-I*^{Tg} mice, suggesting that some form of chronic adaptation may have occurred. In our study, we observed a 2-fold increase in hepatic ABCA1 protein expression in the liver of *hA-I*^{Tg} mice that were wild type for the *Abca1* locus, but no difference was observed for *Abca1* heterozygotes (Fig. 3). These divergent outcomes may result from strain differences in mice between the two studies or other experimental details. The lack of an increase in ABCA1 protein for heterozygous mice in the *hA-I*^{Tg} background suggests that hepatic ABCA1 protein is saturated with bound apoA-I when only one active allele of *Abca1* is present in the mice. Our results suggest that increasing apoA-I concentrations in plasma may protect against atherosclerosis by stabilizing ABCA1 protein at the surface of cells and by providing more substrate (i.e., apoA-I) for HDL particle formation, both of which should stimulate RCT.

We recently reported that liver-specific targeted inactivation of *Abca1* resulted in a profound hypoalphalipoproteinemia and hypercatabolism of apoA-I by the kidney (50). Compared with wild-type mice, liver-specific knockout mice had HDL concentrations that were 20% of normal, a 2-fold increase in plasma removal rate of lipid-free apoA-I or apoA-I in plasma HDL tracer particles, and a corresponding 2-fold increase in kidney degradation of radiolabeled tracer. These results are remarkably similar to those observed in the present study with *Abca1* total knockout mice expressing *hA-I*^{Tg} (Fig. 4, Table 2). Together, our results suggest that the liver is the single most important site of HDL particle assembly and that extrahepatic ABCA1 cannot rescue the hypercatabolism of apoA-I in the absence of hepatic ABCA1. Furthermore, strategies to increase the hepatic expression of ABCA1 protein by increasing the synthesis or decreasing the turnover of ABCA1 protein appear viable possibilities to decrease the risk of premature coronary heart disease.

This work was supported by National Institutes of Health Grants HL-049373 (J.S.P.), HL-054176 (J.S.P.), and HL-07115 (Cardiovascular Pathology Training grant; J.M.T.) and by University of California Department of Energy Contract DE-AC0376SF00098 (Y.Z. and E.M.R.).

REFERENCES

1. Eisenberg, S. 1984. High density lipoprotein metabolism. *J. Lipid Res.* **25:** 1017–1058.
2. Anderson, D. W., A. V. Nichols, T. M. Forte, and F. T. Lindgren. 1977. Particle distribution of human serum high density lipoproteins. *Biochim. Biophys. Acta.* **493:** 55–68.
3. Blanche, P. J., E. L. Gong, T. M. Forte, and A. V. Nichols. 1981. Characterization of human high-density lipoproteins by gradient gel electrophoresis. *Biochim. Biophys. Acta.* **665:** 408–419.
4. Noble, R. P., F. T. Hatch, J. A. Mazrimas, F. T. Lindgren, L. C. Jensen, and G. L. Adamson. 1969. Comparison of lipoprotein analysis by agarose gel and paper electrophoresis with analytical ultracentrifugation. *Lipids.* **4:** 55–59.
5. Cheung, M. C., and J. J. Albers. 1984. Characterization of lipoprotein particles isolated by immunoaffinity chromatography. Particles

containing A-I and A-II and particles containing A-I but no A-II. *J. Biol. Chem.* **259:** 12201–12209.
6. Gordon, D. J., J. L. Probstfield, R. J. Garrison, J. D. Neaton, W. P. Castelli, J. D. Knoke, D. R. Jacobs, Jr., S. Bangdiwala, and H. A. Tyroler. 1989. High-density lipoprotein cholesterol and cardiovascular disease. Four prospective American studies. *Circulation.* **79:** 8–15.
7. Gordon, T., W. P. Castelli, M. C. Hjortland, W. B. Kannel, and T. R. Dawber. 1977. High density lipoprotein as a protective factor against coronary heart disease. The Framingham Study. *Am. J. Med.* **62:** 707–714.
8. Miller, N. E. 1978. The evidence for the antiatherogenicity of high density lipoprotein in man. *Lipids.* **13:** 914–919.
9. Glomset, J. A. 1968. The plasma lecithins:cholesterol acyltransferase reaction. *J. Lipid Res.* **9:** 155–167.
10. Kiss, R. S., D. C. McManus, V. Franklin, W. L. Tan, A. McKenzie, G. Chimini, and Y. L. Marcel. 2003. The lipidation by hepatocytes of human apolipoprotein A-I occurs by both ABCA1-dependent and -independent pathways. *J. Biol. Chem.* **278:** 10119–10127.
11. Attie, A. D., J. P. Kastelein, and M. R. Hayden. 2001. Pivotal role of ABCA1 in reverse cholesterol transport influencing HDL levels and susceptibility to atherosclerosis. *J. Lipid Res.* **42:** 1717–1726.
12. Wang, N., D. Lan, W. Chen, F. Matsuura, and A. R. Tall. 2004. ATP-binding cassette transporters G1 and G4 mediate cellular cholesterol efflux to high-density lipoproteins. *Proc. Natl. Acad. Sci. USA.* **101:** 9774–9779.
13. Yancey, P. G., A. E. Bortnick, G. Kellner-Weibel, M. Llera-Moya, M. C. Phillips, and G. H. Rothblat. 2003. Importance of different pathways of cellular cholesterol efflux. *Arterioscler. Thromb. Vasc. Biol.* **23:** 712–719.
14. Colvin, P. L., E. Moriguchi, P. H. Barrett, J. S. Parks, and L. L. Rudel. 1999. Small HDL particles containing two apoA-I molecules are precursors in vivo to medium and large HDL particles containing three and four apoA-I molecules in nonhuman primates. *J. Lipid Res.* **40:** 1782–1792.
15. Kozarsky, K. F., M. H. Donahee, A. Rigotti, S. N. Iqbal, E. R. Edelman, and M. Krieger. 1997. Overexpression of the HDL receptor SR-BI alters plasma HDL and bile cholesterol levels. *Nature.* **387:** 414–417.
16. Brooks-Wilson, A., M. Marcil, S. M. Clee, L. H. Zhang, K. Roomp, M. van Dam, L. Yu, C. Brewer, J. A. Collins, H. O. Molhuizen, et al. 1999. Mutations in ABC1 in Tangier disease and familial high-density lipoprotein deficiency. *Nat. Genet.* **22:** 336–345.
17. Bodzioch, M., E. Orso, J. Klucken, T. Langmann, A. Bottcher, W. Diederich, W. Drobnik, S. Barlage, C. Buchler, M. Porsch-Ozcurumez, et al. 1999. The gene encoding ATP-binding cassette transporter 1 is mutated in Tangier disease. *Nat. Genet.* **22:** 347–351.
18. Rust, S., M. Rosier, H. Funke, J. Real, Z. Amoura, J. C. Piette, J. F. Deleuze, H. B. Brewer, N. Duverger, P. Denefle, et al. 1999. Tangier disease is caused by mutations in the gene encoding ATP-binding cassette transporter 1. *Nat. Genet.* **22:** 352–355.
19. Lawn, R. M., D. P. Wade, M. R. Garvin, X. Wang, K. Schwartz, J. G. Porter, J. J. Seilhamer, A. M. Vaughan, and J. F. Oram. 1999. The Tangier disease gene product ABC1 controls the cellular apolipoprotein-mediated lipid removal pathway. *J. Clin. Invest.* **104:** R25–R31.
20. Schaefer, E. J., C. B. Blum, R. I. Levy, L. L. Jenkins, P. Alaupovic, D. M. Foster, and H. B. Brewer, Jr. 1978. Metabolism of high-density lipoprotein apolipoproteins in Tangier disease. *N. Engl. J. Med.* **299:** 905–910.
21. Assmann, G., and E. Smootz. 1978. High density lipoprotein infusion and partial plasma exchange in Tangier disease. *Eur. J. Clin. Invest.* **8:** 131–135.
22. Schaefer, E. J., D. W. Anderson, L. A. Zech, F. T. Lindgren, T. B. Bronzert, E. A. Rubalcaba, and H. B. Brewer, Jr. 1981. Metabolism of high density lipoprotein subfractions and constituents in Tangier disease following the infusion of high density lipoproteins. *J. Lipid Res.* **22:** 217–228.
23. Brousseau, M. E., G. P. Eberhart, J. Dupuis, B. F. Asztalos, A. L. Goldkamp, E. J. Schaefer, and M. W. Freeman. 2000. Cellular cholesterol efflux in heterozygotes for Tangier disease is markedly reduced and correlates with high density lipoprotein cholesterol concentration and particle size. *J. Lipid Res.* **41:** 1125–1135.
24. Asztalos, B. F., M. E. Brousseau, J. R. McNamara, K. V. Horvath, P. S. Roheim, and E. J. Schaefer. 2001. Subpopulations of high density lipoproteins in homozygous and heterozygous Tangier disease. *Atherosclerosis.* **156:** 217–225.
25. Wellington, C. L., L. R. Brunham, S. Zhou, R. R. Singaraja, H. Visscher, A. Gelfer, C. Ross, E. James, G. Liu, M. T. Huber, et al. 2003. Alterations of plasma lipids in mice via adenoviral-mediated hepatic overexpression of human ABCA1. *J. Lipid Res.* **44:** 1470–1480.
26. Basso, F., L. Freeman, C. L. Knapper, A. Remaley, J. Stonik, E. B. Neufeld, T. Tansey, M. J. Amar, J. Fruchart-Najib, N. Duverger, et al. 2003. Role of the hepatic ABCA1 transporter in modulating intrahepatic cholesterol and plasma HDL cholesterol concentrations. *J. Lipid Res.* **44:** 296–302.
27. Vaisman, B. L., G. Lambert, M. Amar, C. Joyce, T. Ito, R. D. Shamburek, W. J. Cain, J. Fruchart-Najib, E. D. Neufeld, A. T. Remaley, et al. 2001. ABCA1 overexpression leads to hyperalphalipoproteinemia and increased biliary cholesterol excretion in transgenic mice. *J. Clin. Invest.* **108:** 303–309.
28. Wang, N., D. L. Silver, P. Costet, and A. R. Tall. 2000. Specific binding of apoA-I, enhanced cholesterol efflux, and altered plasma membrane morphology in cells expressing ABC1. *J. Biol. Chem.* **275:** 33053–33058.
29. Remaley, A. T., U. K. Schumacher, J. A. Stonik, B. D. Farsi, H. Nazih, and H. B. Brewer, Jr. 1997. Decreased reverse cholesterol transport from Tangier disease fibroblasts. Acceptor specificity and effect of brefeldin on lipid efflux. *Arterioscler. Thromb. Vasc. Biol.* **17:** 1813–1821.
30. Francis, G. A., R. H. Knopp, and J. F. Oram. 1995. Defective removal of cellular cholesterol and phospholipids by apolipoprotein A-I in Tangier disease. *J. Clin. Invest.* **96:** 78–87.
31. Chajek-Shaul, T., T. Hayek, A. Walsh, and J. L. Breslow. 1991. Expression of the human apolipoprotein A-I gene in transgenic mice alters high density lipoprotein (HDL) particle size distribution and diminishes selective uptake of HDL cholesteryl esters. *Proc. Natl. Acad. Sci. USA.* **88:** 6731–6735.
32. Rubin, E. M., B. Y. Ishida, S. M. Clift, and R. M. Krauss. 1991. Expression of human apolipoprotein A-I in transgenic mice results in reduced plasma levels of murine apolipoprotein A-I and the appearance of two new high density lipoprotein size subclasses. *Proc. Natl. Acad. Sci. USA.* **88:** 434–438.
33. Lee, J. Y., L. Lanningham-Foster, E. Y. Boudyguina, T. L. Smith, E. R. Young, P. L. Colvin, M. J. Thomas, and J. S. Parks. 2004. Prebeta high density lipoprotein has two metabolic fates in human apolipoprotein A-I transgenic mice. *J. Lipid Res.* **45:** 716–728.
34. Paszty, C., N. Mohandas, M. E. Stevens, J. F. Loring, S. A. Liebhaber, C. M. Brion, and E. M. Rubin. 1995. Lethal alpha-thalassaemia created by gene targeting in mice and its genetic rescue. *Nat. Genet.* **11:** 33–39.
35. Sedivy, J. M., and A. L. Joyner. 1992. Gene Targeting. Freeman, New York.
36. Carr, T. P., C. J. Andresen, and L. L. Rudel. 1993. Enzymatic determination of triglyceride, free cholesterol, and total cholesterol in tissue lipid extracts. *Clin. Biochem.* **26:** 39–42.
37. Koritnik, D. L., and L. L. Rudel. 1983. Measurement of apolipoprotein A-I concentration in nonhuman primate serum by enzyme-linked immunosorbent assay (ELISA). *J. Lipid Res.* **24:** 1639–1645.
38. Rainwater, D. L., D. W. Andres, A. L. Ford, W. F. Lowe, P. J. Blanche, and R. M. Krauss. 1992. Production of polyacrylamide gradient gels for the electrophoretic resolution of lipoproteins. *J. Lipid Res.* **33:** 1876–1881.
39. Miller, K. R., J. Wang, M. Sorci-Thomas, R. A. Anderson, and J. S. Parks. 1996. Glycosylation structure and enzyme activity of lecithin:cholesterol acyltransferase from human plasma, HepG2 cells, and baculoviral and Chinese hamster ovary cell expression systems. *J. Lipid Res.* **37:** 551–561.
40. Parks, J. S., A. K. Gebre, and J. W. Furbee, Jr. 1998. Lecithin-cholesterol acyltransferase. Assay of cholesterol esterification and phospholipase A2 activities. In Methods in Molecular Biology. M. Doolittle and K. Reue, editors. Humana Press, Totowa, NJ. 123–131.
41. Wilcox, R. W., T. Thuren, P. Sisson, G. L. Kucera, and M. Waite. 1991. Hydrolysis of neutral lipid substrates by rat hepatic lipase. *Lipids.* **26:** 283–288.
42. Cheung, M. C., and A. C. Wolf. 1988. Differential effect of ultracentrifugation on apolipoprotein A-I-containing lipoprotein subpopulations. *J. Lipid Res.* **29:** 15–25.
43. Kunitake, S. T., and J. P. Kane. 1982. Factors affecting the integrity of high density lipoproteins in the ultracentrifuge. *J. Lipid Res.* **23:** 936–940.
44. McVicar, J. P., S. T. Kunitake, R. L. Hamilton, and J. P. Kane. 1984. Characteristics of human lipoproteins isolated by selected-affinity immunosorption of apolipoprotein A-I. *Proc. Natl. Acad. Sci. USA.* **81:** 1356–1360.

45. McNeish, J., R. J. Aiello, D. Guyot, T. Turi, C. Gabel, C. Aldinger, K. L. Hoppe, M. L. Roach, L. J. Royer, J. de Wet, et al. 2000. High density lipoprotein deficiency and foam cell accumulation in mice with targeted disruption of ATP-binding cassette transporter-1. *Proc. Natl. Acad. Sci. USA.* **97:** 4245–4250.
46. Christiansen-Weber, T. A., J. R. Voland, Y. Wu, K. Ngo, B. L. Roland, S. Nguyen, P. A. Peterson, and W. P. Fung-Leung. 2000. Functional loss of ABCA1 in mice causes severe placental malformation, aberrant lipid distribution, and kidney glomerulonephritis as well as high-density lipoprotein cholesterol deficiency. *Am. J. Pathol.* **157:** 1017–1029.
47. Clifton-Bligh, P., P. J. Nestel, and H. M. Whyte. 1972. Tangier disease. Report of a case and studies of lipid metabolism. *N. Engl. J. Med.* **286:** 567–571.
48. Arakawa, R., and S. Yokoyama. 2002. Helical apolipoproteins stabilize ATP-binding cassette transporter A1 by protecting it from thiol protease-mediated degradation. *J. Biol. Chem.* **277:** 22426–22429.
49. Wang, N., W. Chen, P. Linsel-Nitschke, L. O. Martinez, B. Agerholm-Larsen, D. L. Silver, and A. R. Tall. 2003. A PEST sequence in ABCA1 regulates degradation by calpain protease and stabilization of ABCA1 by apoA-I. *J. Clin. Invest.* **111:** 99–107.
50. Timmins, J. M., J. Y. Lee, E. Boudyguina, K. D. Kluckman, L. R. Brunham, A. Mulya, A. K. Gebre, J. M. Coutinho, P. L. Colvin, T. L. Smith, et al. 2005. Targeted inactivation of hepatic Abca1 causes profound hypoalphalipoproteinemia and kidney hypercatabolism of apoA-I. *J. Clin. Invest.* **115:** 1333–1342.
51. Jauhiainen, M., J. Metso, R. Pahlman, S. Blomqvist, A. van Tol, and C. Ehnholm. 1993. Human plasma phospholipid transfer protein causes high density lipoprotein conversion. *J. Biol. Chem.* **268:** 4032–4036.
52. Pussinen, P., M. Jauhianinen, J. Metso, J. Tyynela, and C. Ehnholm. 1995. Pig plasma phospholipid transfer protein facilitates HDL interconversion. *J. Lipid Res.* **36:** 975–985.
53. Tu, A. Y., H. I. Nishida, and T. Nishida. 1993. High density lipoprotein conversion mediated by human plasma phospholipid transfer protein. *J. Biol. Chem.* **268:** 23098–23105.
54. Barrans, A., X. Collet, R. Barbaras, B. Jaspard, J. Manent, C. Vieu, H. Chap, and B. Perret. 1994. Hepatic lipase induces the formation of pre-beta 1 high density lipoprotein (HDL) from triacylglycerol-rich HDL2. A study comparing liver perfusion to in vitro incubation with lipases. *J. Biol. Chem.* **269:** 11572–11577.
55. Attie, A. D., Y. Hamon, A. R. Brooks-Wilson, M. P. Gray-Keller, M. L. MacDonald, V. Rigot, A. Tebon, L. H. Zhang, J. D. Mulligan, R. R. Singaraja, et al. 2002. Identification and functional analysis of a naturally occurring E89K mutation in the ABCA1 gene of the WHAM chicken. *J. Lipid Res.* **43:** 1610–1617.
56. Schreyer, S. A., L. K. Hart, and A. D. Attie. 1994. Hypercatabolism of lipoprotein-free apolipoprotein A-I in HDL-deficient mutant chickens. *Arterioscler. Thromb.* **14:** 2053–2059.
57. Horowitz, B. S., I. J. Goldberg, J. Merab, T. M. Vanni, R. Ramakrishnan, and H. N. Ginsberg. 1993. Increased plasma and renal clearance of an exchangeable pool of apolipoprotein A-I in subjects with low levels of high density lipoprotein cholesterol. *J. Clin. Invest.* **91:** 1743–1752.
58. Colvin, P. L., and J. S. Parks. 1999. Metabolism of high density lipoprotein subfractions. *Curr. Opin. Lipidol.* **10:** 309–314.
59. Kennedy, M. A., G. C. Barrera, K. Nakamura, A. Baldan, P. Tarr, M. C. Fishbein, J. Frank, O. L. Francone, and P. A. Edwards. 2005. ABCG1 has a critical role in mediating cholesterol efflux to HDL and preventing cellular lipid accumulation. *Cell Metabolism.* **1:** 121–131.
60. Settasatian, N., M. Duong, L. K. Curtiss, C. Ehnholm, M. Jauhiainen, J. Huuskonen, and K. A. Rye. 2001. The mechanism of the remodeling of high density lipoproteins by phospholipid transfer protein. *J. Biol. Chem.* **276:** 26898–26905.
61. Rye, K. A., M. A. Clay, and P. J. Barter. 1999. Remodelling of high density lipoproteins by plasma factors. *Atherosclerosis.* **145:** 227–238.
62. Peterson, J., G. Bengtsson-Olivecrona, and T. Olivecrona. 1986. Mouse preheparin plasma contains high levels of hepatic lipase with low affinity for heparin. *Biochim. Biophys. Acta.* **878:** 65–70.
63. Lambert, G., M. B. Chase, K. Dugi, A. Bensadoun, H. B. Brewer, Jr., and S. Santamarina-Fojo. 1999. Hepatic lipase promotes the selective uptake of high density lipoprotein-cholesteryl esters via the scavenger receptor B1. *J. Lipid Res.* **40:** 1294–1303.
64. de Beer, F. C., P. M. Connell, J. Yu, M. C. de Beer, N. R. Webb, and D. R. van der Westhuyzen. 2000. HDL modification by secretory phospholipase A(2) promotes scavenger receptor class B type I interaction and accelerates HDL catabolism. *J. Lipid Res.* **41:** 1849–1857.
65. Wang, N., and A. R. Tall. 2003. Regulation and mechanisms of ATP-binding cassette transporter A1-mediated cellular cholesterol efflux. *Arterioscler. Thromb. Vasc. Biol.* **23:** 1178–1184.
66. Schmitz, G., and T. Langmann. 2001. Structure, function and regulation of the ABC1 gene product. *Curr. Opin. Lipidol.* **12:** 129–140.
67. Martinez, L. O., B. Agerholm-Larsen, N. Wang, W. Chen, and A. R. Tall. 2003. Phosphorylation of a pest sequence in ABCA1 promotes calpain degradation and is reversed by apoA-I. *J. Biol. Chem.* **278:** 37368–37374.